



OPEN ACCESS

*CORRESPONDENCE

Slobodan M. Todorovic,
✉ slobodan.todorovic@ucdenver.edu

RECEIVED 26 February 2025

ACCEPTED 29 April 2025

PUBLISHED 16 May 2025

CITATION

Timic Stamenic T, Feseha S, Fine-Raquet B, Tadic VP and Todorovic SM (2025) *In vivo* silencing of the thalamic $\text{Ca}_v3.1$ voltage-gated calcium channels demonstrates their region-specific role in anesthetic mediated hypnosis. *Exp. Biol. Med.* 250:10553. doi: 10.3389/ebm.2025.10553

COPYRIGHT

© 2025 Timic Stamenic, Feseha, Fine-Raquet, Tadic and Todorovic. This is an open-access article distributed under the terms of the [Creative Commons Attribution License \(CC BY\)](https://creativecommons.org/licenses/by/4.0/). The use, distribution or reproduction in other forums is permitted, provided the original author(s) and the copyright owner(s) are credited and that the original publication in this journal is cited, in accordance with accepted academic practice. No use, distribution or reproduction is permitted which does not comply with these terms.

In vivo silencing of the thalamic $\text{Ca}_v3.1$ voltage-gated calcium channels demonstrates their region-specific role in anesthetic mediated hypnosis

Tamara Timic Stamenic¹, Simon Feseha¹, Brier Fine-Raquet¹, Vasilije P. Tadic¹ and Slobodan M. Todorovic^{1,2,3*}

¹Department of Anesthesiology, University of Colorado, Aurora, CO, United States, ²Department of Neuroscience, University of Colorado, Aurora, CO, United States, ³Department of Pharmacology Graduate Programs, University of Colorado, Aurora, CO, United States

Abstract

Although substantial progress has been made in the last three decades towards our understanding of how general anesthetics (GAs) act at the molecular level, much less is known about how GAs cause loss of consciousness at the level of neuronal networks. The role of thalamus as an important brain region in anesthetic-induced hypnosis is relatively well established, but the specific roles of voltage-gated ion channels in different functional regions of the thalamus in anesthetic mechanisms are not well studied. To address this gap in knowledge, we selectively silenced the *Cacna1g* gene that encodes the low-threshold-activated $\text{Ca}_v3.1$ T-type voltage-gated calcium channel subunit by injecting short-hairpin RNA (shRNA) into midline and intralaminar - nonspecific thalamus (MIT) and sensory - specific ventrobasal (VB) thalamic nuclei in wild-type (WT) mice. Control animals were injected with scrambled shRNA. To validate our silencing approach, we performed patch-clamp experiments in acute thalamic slices *ex vivo*. In injected animals we determined anesthetic endpoints such as hypnosis measured with loss of righting reflex (LORR) and immobilization measured with loss of withdrawal reflex (LOWR) *in vivo* after administration of a traditional volatile GA isoflurane. Effective $\text{Ca}_v3.1$ channel knock-down was documented by greatly diminished amplitudes of T-currents and absence of rebound burst firing in our patch-clamp recordings from thalamic slices. We found that knocking down $\text{Ca}_v3.1$ channels in MIT significantly decreased inhaled isoflurane concentration that is required to induce LORR, but it did not affect speed of anesthetic induction and the immobilizing effect of isoflurane. In contrast, knocking down the $\text{Ca}_v3.1$ channel in the VB thalamus did not affect any of the measured

anesthetic endpoints. Hence, we concluded that $\text{Ca}_v3.1$ channels in nonspecific MIT thalamus have a preferential role in anesthetic hypnosis when compared to the sensory VB thalamus.

KEYWORDS

calcium ion channels, thalamus, anesthesia, isoflurane, hypnosis

Impact Statement

General anesthetics (GAs) have been clinically used for nearly two centuries, but the mechanisms whereby different classes of these agents achieve different clinical effects are still not well understood. We found that knocking down $\text{Ca}_v3.1$ channels in MIT significantly decreased inhaled isoflurane concentration that is required to induce LORR, but it did not affect speed of anesthetic induction and immobilizing effect of isoflurane. In contrast, knocking down $\text{Ca}_v3.1$ channel in the VB thalamus did not affect any of the measured anesthetic endpoints.

Introduction

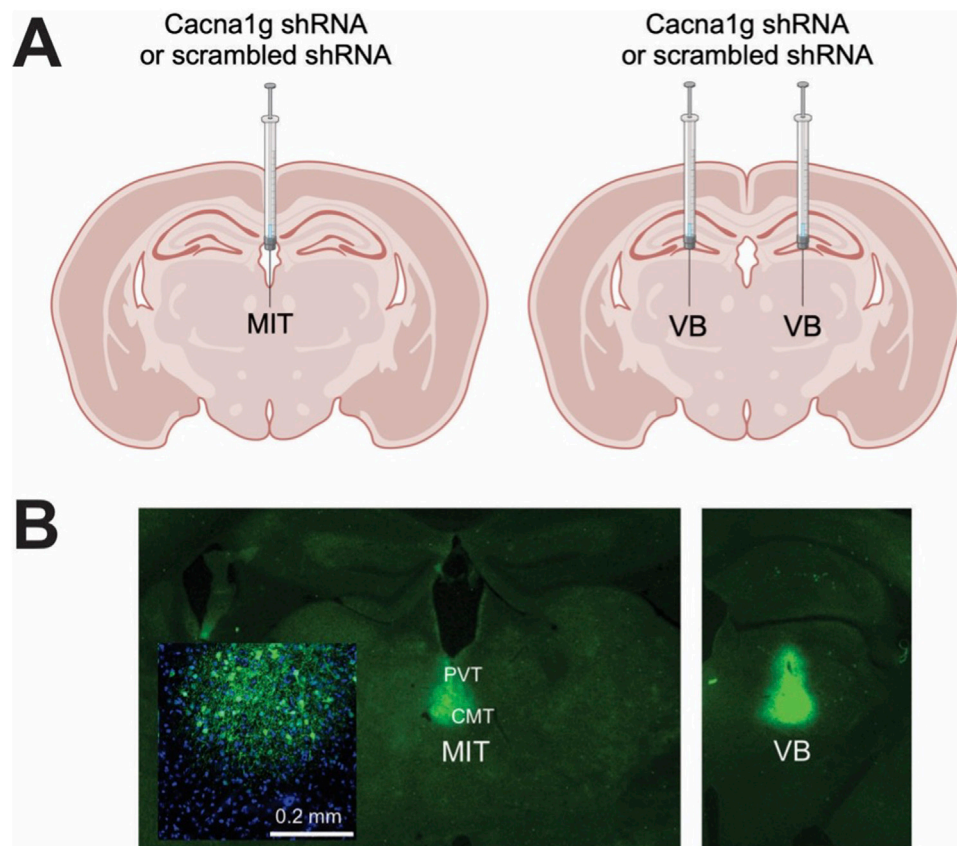
General anesthetics (GAs) have been clinically used for nearly two centuries, but the mechanisms whereby different classes of these agents achieve different clinical effects are still not well understood. A complete anesthetic state involves loss of consciousness (hypnosis) and movement (immobilization), as well as loss of both pain sensation (analgesia) and recollection of the event (amnesia). Research advances in the last three decades strongly suggest that GAs act through specific sites on the neuronal membrane and that different ion channels that control neuronal excitability may mediate their clinical effects [1, 2]. It is well known that most GAs currently in use have either N-methyl-D-aspartate (NMDA) receptor-blocking or/and γ -aminobutyric acid A (GABA_A) receptor-mimetic properties that can account for anesthetic hypnosis [1]. However, a family of neuronal voltage-gated calcium channels (VGCCs) was also implicated in the mechanisms of anesthesia because VGCC inhibition may be important in anesthetic action by decreasing neuronal excitability and presynaptic excitatory transmission [3].

Thalamus is one of the brain regions implicated in regulation of arousal, natural sleep-wake cycle and a very relevant site of anesthetic actions. The thalamus has traditionally been divided into three anatomical and functional groups: the principal (relay, sensory or motor) nuclei, the association nuclei, and the midline and intralaminar nuclei (MIT) [4, 5]. Since the sensory nuclei receive sensory information through ascending pathways and transmit it to distinct regions of the cortex, they are known as a specific part of thalamus [4, 5]. On the other hand, MIT are historically known as a nonspecific thalamus because of diffuse

projections to different cortical and subcortical areas [4, 5]. Various thalamic nuclei are important in awareness, cognitive functions, and as targets for many GAs [1, 6, 7]. Importantly, most thalamic nuclei express different isoforms of T-type VGCCs that activate with small membrane depolarizations. The T-channels are crucial for the rhythmic oscillations between mutually interconnected cortical, inhibitory GABAergic neurons in the nucleus reticularis thalami (nRT) and glutamatergic relay neurons in the sensory thalamic nuclei (VB) and MIT. Our previous studies established that nRT neurons are enriched in $\text{Ca}_v3.2$ and $\text{Ca}_v3.3$ isoforms of T-channels that underlie their low-threshold-calcium spikes (LTs) and burst firing [8]. In contrast to nRT, neurons of the VB and MIT express almost exclusively the $\text{Ca}_v3.1$ isoform of T-channels [9–11]. In addition, we reported that $\text{Ca}_v2.3$ R-type of VGCCs is also expressed in central medial nucleus of the thalamus (CMT, part of intralaminar thalamus) and in concert with the $\text{Ca}_v3.1$ T-type channels regulate neuronal excitability [11, 12].

Recent findings have suggested that the intralaminar parts of thalamus (CMT) may act as a key hub through which GA-induced hypnosis and natural sleep are initiated [6]. Additionally, the CMT has been identified as the neuroanatomical site mediating the arousal response by manipulating activity of voltage-gated potassium channels [13–15]. Moreover, studies demonstrated that the paraventricular thalamus (PVT, part of the midline thalamus), is a key wakefulness-controlling nucleus in the thalamus [16, 17]. However, despite the proposed roles of the CMT and PVT in regulation of the state of arousal, the ability of GAs to regulate activity of VGCCs and specifically $\text{Ca}_v3.1$ channels in MIT in the context of anesthetic endpoints is not well established.

We previously reported that T-currents in the CMT, nRT and VB are inhibited by clinically relevant concentrations of volatile GAs [11, 18, 19]. This strongly suggests that thalamic T-currents participate in anesthetic action, however, new genetic tools are needed for proof-of-concept studies for the role of T-channels in the clinical effects of GAs. Further, potential region-specific differences of T-channel inhibition within the thalamus are not known. To address this gap in knowledge, here we selectively silenced the *Cacna1g* gene that encodes the $\text{Ca}_v3.1$ T-channel subunit by injecting short-hairpin RNA (shRNA) [20] into MIT and VB thalamic nuclei in wild-type (WT) mice. We then determined anesthetic endpoints such as

**FIGURE 1**

Generation of selective thalamic $\text{Ca}_v3.1$ T-channels knock-down mice. **(A)** Diagram of stereotaxic injections; control (scrambled shRNA) or *Cacna1g* shRNA injection in the non-specific thalamus (midline and intralaminar thalamus - MIT) or specific – sensory thalamus (ventrobasal thalamus - VB). **(B)** Stereotaxic injections confirmation by immunohistochemistry.

hypnosis and immobilization after administration of a traditional volatile GA isoflurane.

Materials and methods

To investigate the potential role of thalamic T-channels in anesthesia, we used a methodology which silences the *Cacna1g* gene that encodes the $\text{Ca}_v3.1$ channel pore-forming subunit by injecting short-hairpin RNA (shRNA); this is the same procedure employed by others [21] and in our recent study [20]. In short, high-titer AAV2 vectors expressing $\text{Ca}_v3.1\text{shRNA}$ (AAV2-GFP-U6-*mCACNA1G-shRNA*) or control (scrambled shRNA) were obtained from Vector BioLabs, prepared and delivered either into the MIT targeting the intralaminar (CMT) and midline parts of thalamus (PVT) (in mm from bregma, AP: -1.35 , ML: 0 , DV: 3.95) or targeting both the right and left VB thalamus (AP: -1.75 , ML: ± 1.60 , DV: 4.00) of WT male mice by stereotaxic injections using a $5\text{-}\mu\text{L}$ Hamilton syringe at a rate of $0.1\text{ }\mu\text{L}/\text{min}$. Figure 1 shows a schematic of

these areas. The induction of anesthesia in mice was performed in an anesthesia chamber with 3% isoflurane, after which they were placed on a stereotaxic frame and kept anesthetized via nose cone that continuously delivered 2-3% isoflurane throughout the whole procedure. Mice were monitored for the changes in the respiratory rate and the concentration of isoflurane was adjusted accordingly. The frame was equipped with automated drilling, followed by ultraprecise injection (Robot Stereotaxic, Neurostar). After surgery mice were treated with the analgesic Banamine 2 days and allowed to recover if no major neurological deficits were noticed. The effects of *Cacna1g* shRNA or control (scrambled shRNA) were studied at least 2 weeks following injections to allow adequate time for virus spread in the targeted areas.

Immunohistochemistry (IHC)

Following completion of behavioral experiments, brains of all mice injected with *Cacna1g* shRNA or scrambled shRNA were

processed for localization verification. Mice were deeply anesthetized with 5% isoflurane and transcardially perfused with phosphate buffered saline (PBS pH 7.4, Life Technologies), followed by 4% paraformaldehyde in 0.1 M phosphate buffer, pH 7.4 (PFA). Whole brains were extracted and post-fixed in PFA for 24 h. Brains were rinsed in PBS, embedded in 3% agarose and brain sections (50 μ m) were prepared on a microtome (Leica VT1200). Slices were rinsed three times in PBS, mounted on slides and an antigen retrieval process was performed by exposing slides to a boiling citric buffer solution (0.1 M, pH 6.0). Sections were permeabilized in 1% glycine in PBST for 15 min and rinsed in PBS for 5 min. Sections were then blocked with 5% normal donkey serum in PBST (0.1% Triton X-100 in PBS) for 30 min, and incubated with primary antibody (rabbit anti-GFP; 1:1000; A11122; Invitrogen) diluted in 1% normal donkey serum in PBST overnight at 4°C. Slices were rinsed 3 \times 5 min in PBST followed by a 5-min rinse in PBS and then incubated for 2 h with secondary anti-rabbit antibody (anti-rabbit Alexa 488: 1:500, Invitrogen) at room temperature and washed 3 \times 5 min in PBS. Sections were coverslipped using a fluorescent mounting medium containing DAPI (Vector laboratories) and images were taken using a confocal laser scanning microscope (Olympus FluoView FV1200) at \times 20 magnification using image stitching to obtain the entire region of interest. Although, in our stereotaxic injections we targeted the CMT, we found using confocal microscopy that GFP immunofluorescence has spread into adjacent nuclei [PVT and/or interomediodorsal nucleus of thalamus (IMD), Figure 1] in most of our experiments. Hence, due to this technical limitation we refer to nonspecific thalamic injections as targeting MIT, not just CMT. Only the mice that had viral GFP expression localized to the MIT or VB were included in analysis.

Brain slice preparation for patch-clamp electrophysiology experiments

Patch-clamp experiments using brain slices from the virus-injected mice began at least 2 weeks after injection. Animals were anesthetized briefly with isoflurane, decapitated, and their brains rapidly removed. Fresh horizontal brain slices, 250 μ m-thick, were sectioned at 4°C in a pre-chilled solution containing (in mM): sucrose 260, D-glucose 10, NaHCO₃ 26, NaH₂PO₄ 1.25, KCl 3, CaCl₂ 2, MgCl₂ 2, using a vibrating micro slicer (Leica VT 1200S). Brain slices were immediately incubated for 45 min in a solution containing (in mM): NaCl 124, D-glucose 10, NaHCO₃ 26, NaH₂PO₄ 1.25, KCl 4, CaCl₂ 2, MgCl₂ 2 at 37°C prior to use in electrophysiology experiments, which were conducted at room temperature. During incubation, slices were constantly perfused with a gas mixture of 95% O₂ and 5% CO₂ (v/v).

Patch-clamp electrophysiology recordings

The external solution for whole-cell voltage-clamp recordings consisted of (in mM): NaCl 125, D-glucose 25, NaHCO₃ 25, NaH₂PO₄ 1.25, KCl 2.5, MgCl₂ 1, and CaCl₂ 2. This solution was equilibrated with a mixture of 95% O₂ and 5% CO₂ (v/v) for at least 30 min with a resulting pH of approximately 7.4. The internal solution for recording well isolated T-currents consisted of (in mM): tetramethyl ammonium (TMA)-OH 135, EGTA 10, MgCl₂ 2, and HEPES 40, titrated to pH 7.2 with hydrofluoric acid (HF) [22].

The current-voltage (I-V) curves were generated by stepping from the holding potential (V_h) of -90 mV to depolarized test potentials (V_t) from -80 to -40 mV in 2.5 mV increments. The voltage dependencies of steady-state activation were described with single Boltzmann distributions of the following forms: Activation: $G(V) = G_{\max} / (1 + \exp[-(V - V_{50})/k])$; G_{\max} is the maximal conductance (calculated by dividing current amplitude by estimated reversal potential), V_{50} is the voltage at which half of the current is activated, and k represents the voltage dependence (slope) of the distribution. The T-currents from the inactivation protocol were recorded by using a standard double-pulse protocol with 3.6-s-long prepulses to variable voltages (from -120 to -60 mV in 5 mV increments) and test potentials to -50 mV.

For the whole-cell current-clamp recordings, the internal solution consisted of (in mM): potassium-D-gluconate 130, EGTA 5, NaCl 4, CaCl₂ 0.5, HEPES 10, Mg ATP 2, Tris GTP 0.5, pH 7.2. Glass micropipettes (Sutter Instruments O.D. 1.5 mm) were pulled using a Sutter Instruments Model P-1000 and fabricated to maintain an initial resistance of 3–5 M Ω . GFP-expressing thalamic neurons were identified using the microscope with epifluorescence and IR-DIC optics. Intrinsic excitability of thalamic neurons was characterized by using a multi-step protocol which consisted of injecting a family of depolarizing (50–300 pA) current pulses of 400 ms duration in 25 pA increments followed by a series of hyperpolarizing currents of the same duration stepping from -50 to -250 pA in 25 pA increments. Subsequent action potential (AP) tonic and rebound firing frequencies (per pulse and per burst) and input resistances were determined. The membrane potential was measured at the beginning of each recording and was not corrected for the liquid junction potential, which was around 10 mV in our experiments. The membrane input resistance was calculated by dividing the end of steady-state hyperpolarizing voltage deflection by the injected current. Neuronal membrane responses were recorded using a Multiclamp 700B amplifier (Molecular Devices, CA, United States). Voltage current commands and digitization of the resulting voltages and currents were performed with Clampex 8.3 software

(Molecular Devices), and voltage and current traces were analyzed using Clampfit 10.5 (Molecular Devices).

Animals

Experimental procedures with animals were performed according to the guidelines approved by the Institutional Animal Care and Use Committee (IACUC) of the University of Colorado Anschutz Medical Campus. Treatments of animals adhered to guidelines set forth in the NIH Guide for the Care and Use of Laboratory Animals. Our study was approved by the ethics committee of the University of Colorado Anschutz Medical Campus. The adult male C57BL/6J wild type (WT) mice (between 2 and 4 months of age) were used for behavioral experiments. C57BL/6J mice were obtained from the Jackson laboratory (USA). We opted for male mice, as very little is known about sex differences in activity of volatile anesthetics in the thalamus. All animals were maintained on a 14/10 h light-dark cycle with food and water *ad libitum*. Anesthetic endpoints were measured as we previously reported [23] as follows.

Loss of righting reflex (LORR) and loss or withdrawal reflex (LOWR)

LORR is assessed by placing the mouse on its back until animal loses righting reflex. The criterion for the LORR is failure of mouse to right within a 30-s period. For LOWR, an alligator clip covered with airway tubing was used on proximal 1/3 tail and LOWR was considered when there was no withdrawal for a minimum of 30-s. All mice were placed on a heating pad in a chamber equilibrated with 0.5% isoflurane. Isoflurane was then increased by 0.1% every 10 min until LORR and LOWR was obtained. Illustration of the experiments with LORR and LOWR determination is depicted on top panels of Figures 4A, 5A.

Anesthetic induction

Induction time was assessed by measuring the time to LORR (TTLORR) at a constant inhaled concentration of 1.2% isoflurane. Mice were placed on the heating pad in anesthetic chamber that was set at 1.2% isoflurane after a 30-min wait. Successful induction was determined when a mouse failed to right within a 30-s period.

Drugs

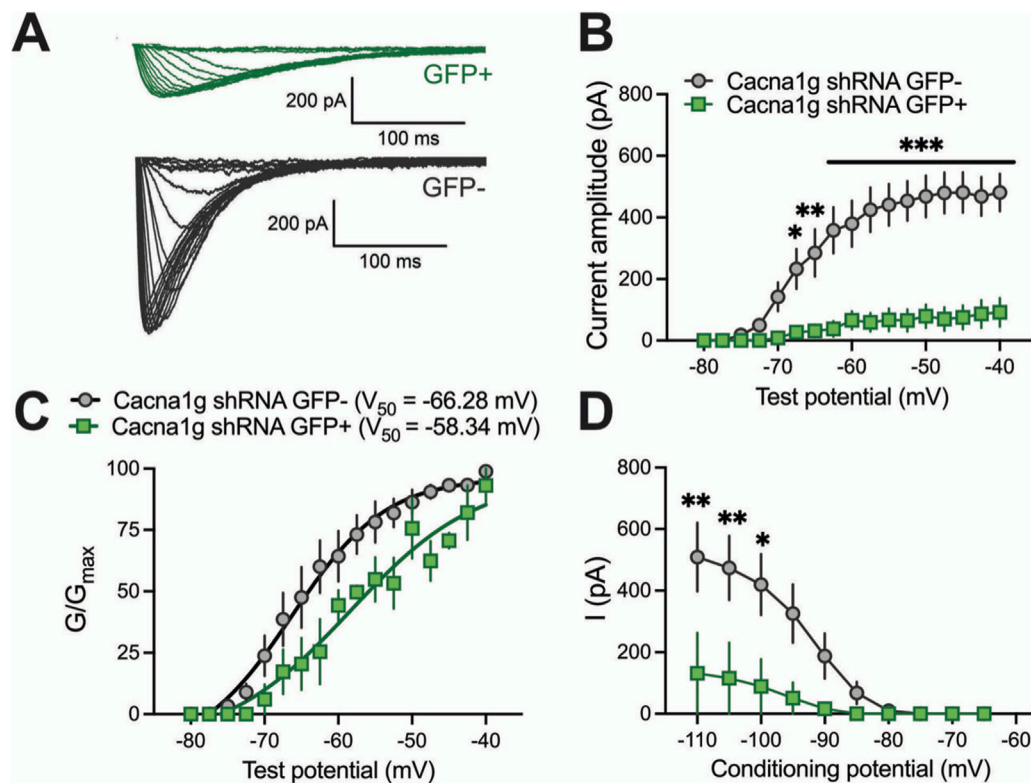
Isoflurane was purchased from McKesson (San Francisco, CA) and Banamine (Merck) was obtained from the University of Colorado Hospital pharmacy.

Data analysis

In every experiment, we attempted to minimize the number of animals used. All animals with complete data set and physiological parameters were included in the study. Statistical analysis was performed using two-way repeated measure (RM) ANOVA as well as student unpaired and two-tailed *t*-test, where appropriate. We used *Sidak's multiple comparisons test* where interaction between factors after two-way RM ANOVA was significant. Significance was accepted with *p* values < 0.05. Statistical and graphical analysis was performed using GraphPad Prism 8.00 software (GraphPad Software, La Jolla, CA, United States) and Origin 2018 (OriginLab, Northampton, MA, United States).

Results

To validate functional knock-down of T-currents we first performed patch-clamp recordings using acute brain slices from WT mice injected with *Cacna1g* shRNA (Figure 2). Transfected neurons were readily identified in our recordings from live brain slices with bright GFP immunofluorescence. Specifically, we compared T-current biophysical properties from the acute thalamic slices in GFP positive (GFP+) and GFP negative (GFP-) neurons. T-currents were evoked using our standard current-voltage (I-V) protocols with depolarizing steps to test potentials (*V_t*) from −80 to −40 mV from holding (*V_h*) potentials of −90 mV. Original traces of inward calcium currents from representative recordings in the CMT in GFP+ neurons (green traces) and GFP- neurons (black traces) are depicted in Figure 2A. On average, we found that peak T-currents in GFP+ neurons (*n* = 7, green symbols) were almost completely abolished as evidenced by about 90% decreased amplitudes when compared to GFP- neurons (*n* = 7, gray symbols) across most of the test potentials in our I-V recordings (Figure 2B). We next compared steady-state activation curves in two groups and found that GFP+ neurons exhibited a small but insignificant depolarizing shift in *V₅₀* of channel activation when compared to GFP- neurons (Figure 2C). Finally, we used an independent protocol of recordings T-current amplitudes (*V_t* −50 mV) after conditioning pre-pulses from −110 to −60 mV. Average graphs from these experiments showing largely decreased T-current amplitudes in GFP+ neurons (green symbols) when compared to GFP- neurons (gray symbols) is summarized on Figure 2D. Our results showing greatly decreased T-current amplitudes strongly suggest that excitability of GFP+ neurons may be decreased as result of injections of *Cacna1g* shRNA. Hence, in ensuing current-clamp experiments we compared tonic and burst firing properties of GFP+ and GFP- neurons in CMT as summarized on Figure 3. Original traces of a rebound action potential (AP) and a T-channel-dependent low-threshold-calcium spike (LTS) from a GFP- neuron (gray trace) are

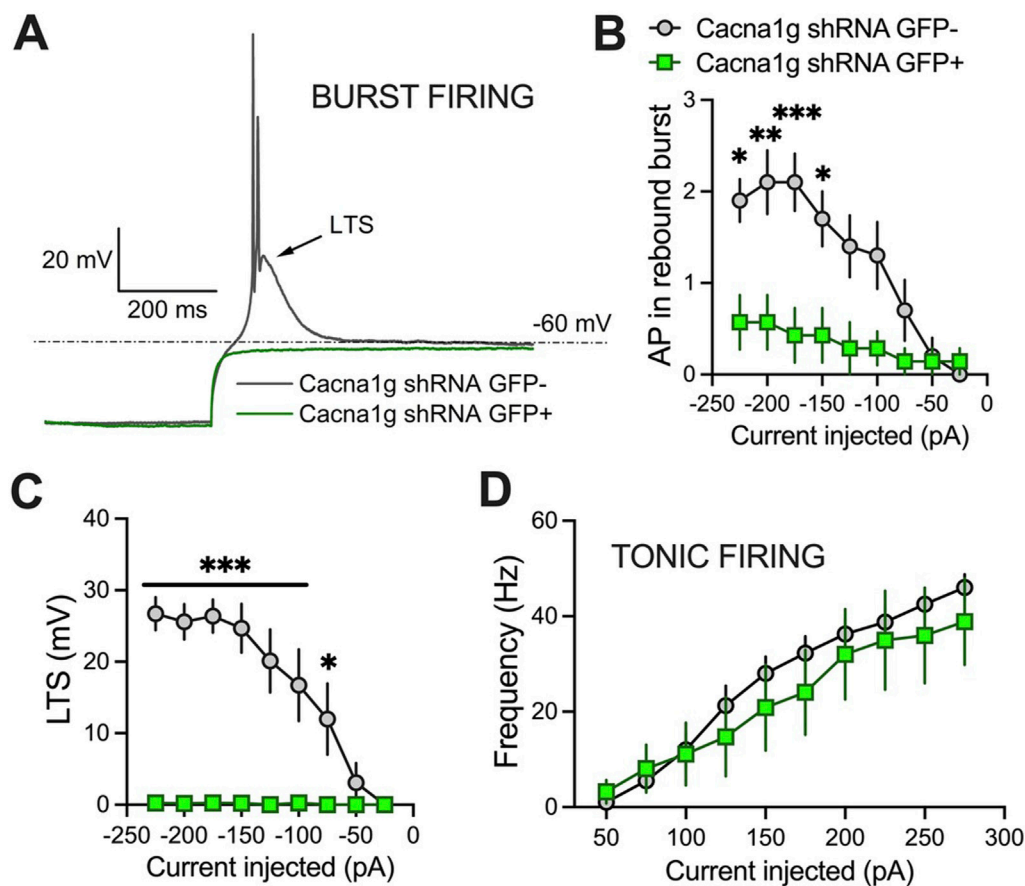
**FIGURE 2**

Biophysical properties of thalamic T-currents in *Cacna1g* shRNA GFP+ and GFP- neurons. **(A)** T-current $I-V$ traces from representative GFP+ (green) and GFP- (black) neurons in the voltage range for V_t of -80 to -40 mV from an initial holding potential (V_h) of -90 mV in 2.5 mV increments. Note that the T-currents recorded from the GFP+ cells are smaller and don't show typical criss-crossing pattern. **(B)** Average T-current amplitude, as calculated from the steady-state activation protocol was reduced in *Cacna1g* shRNA GFP+ neurons in comparison to GFP- cells (two-way RM ANOVA: interaction $F_{(16,129)} = 12.54$, $p < 0.001$; test potential $F_{(16,192)} = 25.01$, $p < 0.001$, GFP $F_{(1,12)} = 27.34$, $p < 0.001$; Sidak's *post hoc* presented on Figure). $N = 7$ cells per group, note that 3 GFP+ cells did not have T-currents. **(C)** The average voltage dependence of a steady-state activation (G/G_{max}) curve with V_{50} value noted on the graph for GFP+ and GFP- thalamic neurons. The difference between V_{50} for T-current activation was not statistically significant between GFP+ and GFP- cells. $N = 3$ GFP+, $N = 7$ GFP- neurons. **(D)** Average T-current amplitude, as calculated from the steady-state inactivation protocol (double-pulse protocol with 3.6 -s-long prepulses to variable voltages (from -120 to -50 mV in 5 mV increments) and a test potential (V_t) of -50 mV) was greatly reduced in *Cacna1g* shRNA GFP+ neurons in comparison to GFP- cells (two-way RM ANOVA: interaction $F_{(9,72)} = 4.61$, $p < 0.001$; potential $F_{(9,72)} = 12.24$, $p < 0.001$, GFP $F_{(1,8)} = 4.99$, $p = 0.056$; Sidak's *post hoc* presented on Figure). $N = 4$ GFP+, $N = 6$ GFP- cells per group, note that just one of four GFP+ cells had measurable T-currents. * $p < 0.05$, ** $p < 0.01$, *** $p < 0.001$.

depicted on Figure 3A. The same figure shows a lack of rebound APs and completely abolished LTS in a GFP+ neuron (green trace). In the summary graph on Figure 3B we depict the average number of rebound APs in GFP- neurons ($n = 10$ neurons, gray symbols) resulting from progressively stronger hyperpolarizing steps from -50 to -250 pA. In contrast, the same figure shows only minimal active membrane response upon injections of the same currents ($n = 7$ neurons, gray symbols). Likewise, Figure 3C shows that in the same two groups when we compared LTSs are completely absent in GFP+ neurons (green symbols) while in GFP- neurons (gray symbols) they show typical voltage-dependence with larger amplitudes associated with stronger current injections. As expected, we found very little difference in the two groups when we compared properties of tonic firing of APs in response to escalating depolarizing current injections from $+50$ to $+300$ pA (Figure 3D). Overall, our patch-clamp

recordings from thalamic neurons *ex vivo* in animals injected with *Ca v 3.1*shRNA show that GFP+ neurons exhibited largely decreased T-current amplitudes and greatly diminished rebound burst firing.

In the ensuing *in vivo* experiments, we tested control groups (mice injected with scrambled shRNA) and experimental groups (mice injected with *Cacna1g* shRNA) for anesthetic endpoints, as determined by concentrations of inhaled isoflurane required to induce LORR. The examiner was blinded to the experimental and control groups. Figure 4 summarizes our data from the experiments where the *Cacna1g* shRNA or scrambled shRNA (control group) were injected into MIT. We found no significant difference in speed of induction as measured by TTLORR in *Cacna1g* shRNA group ($n = 6$, green symbols) when compared to our controls ($n = 8$, scrambled shRNA, gray symbols) as depicted on Figure 4B. In

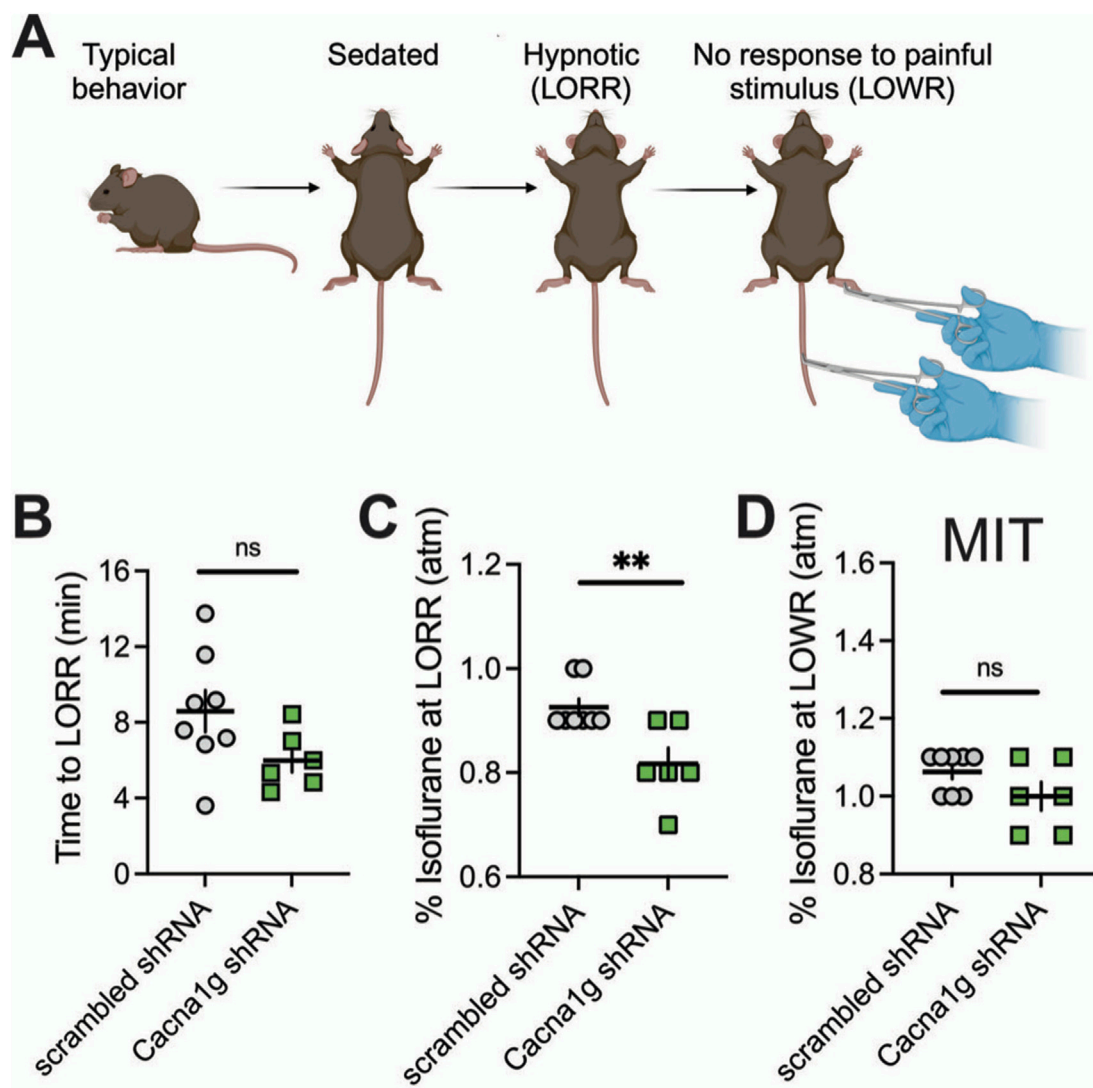
**FIGURE 3**

Excitability differences between GFP+ and GFP- thalamic neurons from *Cacna1g* shRNA injected animals. **(A)** Original traces from representative thalamic neurons recorded from GFP+ (green) and GFP- (gray) neurons show active membrane responses to a hyperpolarizing (−225 pA) current injection. Note that GFP+ neuron does not show APs nor low threshold spike (LTS) after membrane hyperpolarization. **(B)** Number of action potentials (AP) in rebound burst was statistically significant smaller in GFP+ neurons (two-way RM ANOVA: interaction $F_{(8,120)} = 5.34$, $p < 0.001$; current injected $F_{(8,120)} = 11.95$, $p < 0.001$, GFP $F_{(1,15)} = 9.07$, $p = 0.009$; Sidak's *post hoc* presented on Figure). **(C)** LTS was not observed in GFP+ neurons (two-way RM ANOVA: interaction $F_{(8,120)} = 12.06$, $p < 0.001$; current injected $F_{(8,120)} = 12.51$, $p < 0.001$, GFP $F_{(1,15)} = 31.07$, $p < 0.001$; Sidak's *post hoc* presented on Figure). **(D)** Graph of averages of tonic AP firing frequency and current injections of 50–275 pA from multiple experiments shows no difference between GFP+ and GFP- *Cacna1g* shRNA injected thalamic neurons. $N = 7$ GFP+, $N = 10$ GFP- cells. * $p < 0.05$, ** $p < 0.01$, *** $p < 0.001$.

contrast, we found about 10% decrease in inhaled % atm isoflurane needed to induce LORR in group where *Cacna1g* shRNA was injected in the MIT region (Figure 4C). Finally, we found that the immobilizing effect measured by LOWR after injections of *Cacna1g* shRNA and scrambled shRNA into MIT region was not different in the two groups (Figure 4D). In contrast, mice injected with *Cacna1g* shRNA in the VB region ($n = 9$) did not show any difference in the speed of anesthetic induction (Figure 5B), or concentration of isoflurane required to induce LORR when compared to controls ($n = 9$) (Figure 5C). Similarly to injections to MIT, we found that LOWR response was not different between *Cacna1g* shRNA ($n = 9$) and scrambled shRNA ($n = 9$) group in our VB injections (Figure 5D). We conclude that *in vivo* silencing of $Ca_v3.1$ channels in two functionally different regions of the

thalamus, such as the MIT and the VB, differentially affected the required hypnotic concentration of isoflurane without an apparent difference in the speed of anesthetic induction and immobilizing properties of isoflurane.

In the ensuing *in vivo* experiments, we also tested the ability of mice injected either with scrambled shRNA or with *Cacna1g* shRNA into the MIT or the lateral thalamus targeting bilateral VB to perform behavioral tasks in an open-field test. We found that performance of mice during 10 min of testing in the groups injected either with scrambled or *Cacna1g* shRNA when compared to the naive, uninjected mice, was not different in the open-field testing ($n = 5$ – 10 mice per group, data not shown). Hence, it appears that intrathalamic injection of viral vectors did not cause any major neurological deficit *per se* because it did not affect the general motor ability of mice.

**FIGURE 4**

Effect of knocking-down of $Ca_v3.1$ T-channels from MIT on LORR. (A) Schematic representation of LORR and LOWR experiments. (B) Time to LORR was not statistically significant between control (scrambled shRNA) and Cacna1g shRNA MIT injected mice. (C) Cacna1g shRNA MIT injected animals required less isoflurane for achieving LORR (hypnotic effect) in comparison to control male mice (unpaired two-tailed t-test: $t_{(12)} = 3.34$, $p = 0.006$). (D) There was no difference in isoflurane requirement for LOWR between control scrambled shRNA and Cacna1g shRNA MIT injected animals. $N = 8$ control scrambled shRNA and $N = 6$ Cacna1g shRNA animals. ** $p < 0.01$.

Discussion

One of the compelling reasons to study VGCCs in the mechanisms of anesthetic actions is that these channels are essential in regulation of synaptic transmission and excitability in the neuronal sleep pathway such as thalamus. The thalamus is the major gateway for the flow of sensory information from the periphery to the cortex and the disruption of thalamocortical connectivity may be an essential common feature of the hypnotic effects of many GAs. Indeed, both human and animal studies *in vivo* have indicated that the thalamus is deactivated during anesthesia [24]. Two thalamic

regions are particularly relevant for our considerations as neuronal network targets for GAs. One such region, the thalamic VB nucleus, receives direct sensory projections from the periphery and projects mostly to the barrel cortex, it is a principal thalamic nucleus often referred to as a specific or sensory thalamus [5, 25]. The other region of interest, known as a nonspecific thalamus, consists of the CMT and PVT, parts of the MIT, which project diffusely to the different cortical and subcortical areas [5]. The parts of MIT are interposed between the brain stem “arousal” system and are ideally suited to control the overall level of thalamic and cortical activity [5, 26, 27]. Importantly, our previous *ex vivo* studies using acute brain slices

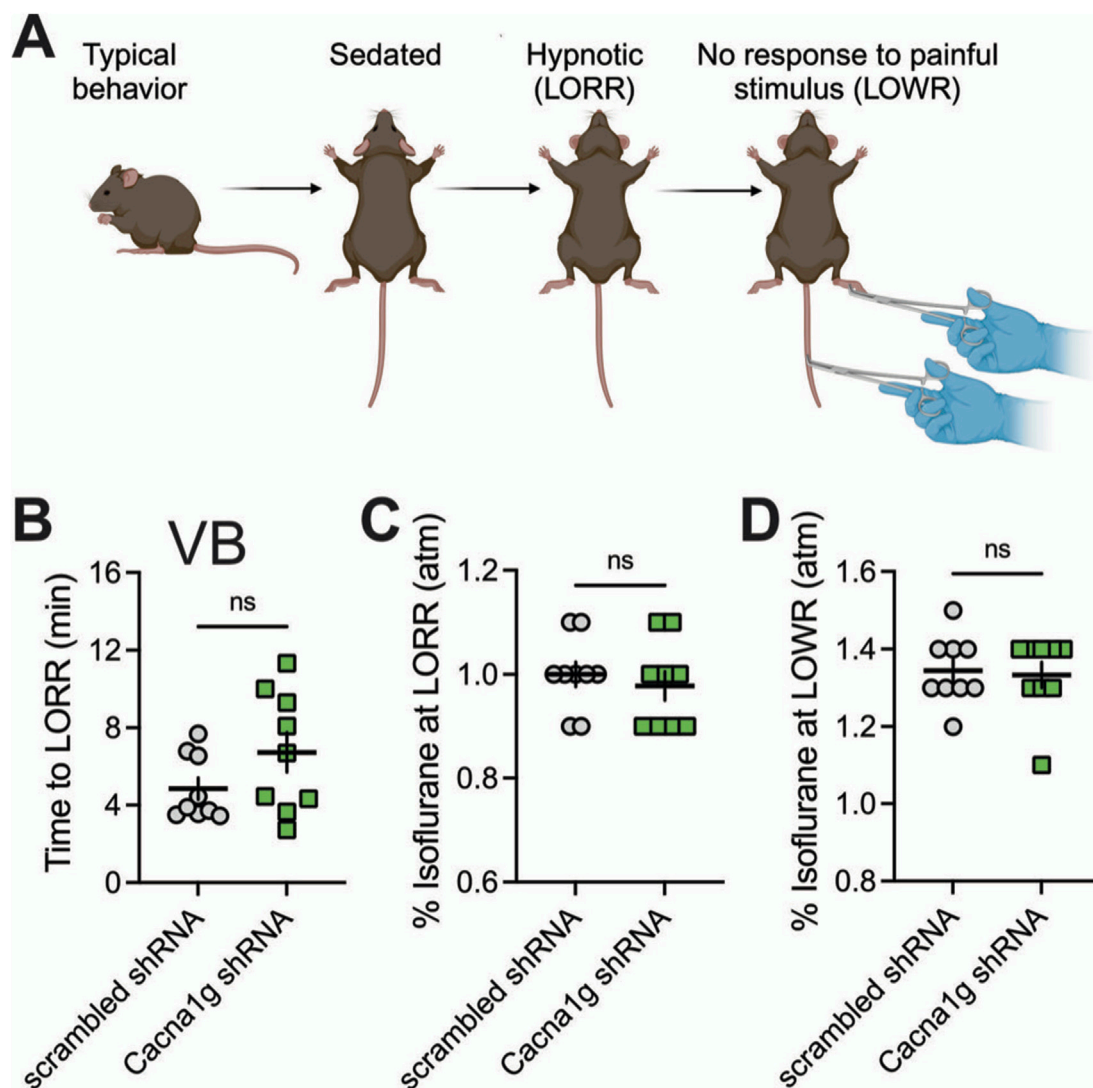


FIGURE 5

Effect of knocking-down of $\text{Ca}_v3.1$ T-channels from VB on LORR. (A) Schematic representation of LORR and LOWR experiments. (B) Time to LORR was not statistically significant between control (scrambled shRNA) and *Cacna1g* shRNA in VB injected mice. (C) There was no difference in isoflurane requirement for LORR (hypnotic effect) between control and *Cacna1g* shRNA in VB injected mice. (D) There was no difference in isoflurane requirement for LOWR between control and *Cacna1g* shRNA in VB injected animals. N = 9 control scrambled shRNA and N = 9 *Cacna1g* shRNA animals.

have demonstrated that $\text{Ca}_v3.1$ channel-mediated excitability in both the VB [19] and in the CMT [11] is diminished with clinically relevant concentrations of isoflurane. Hence, we hypothesized that knocking-down $\text{Ca}_v3.1$ channels in the CMT and VB neurons may have different effects on loss of consciousness induced by GAs. To test this hypothesis, we produced region-specific knock-down of $\text{Ca}_v3.1$ channels in MIT and VB nuclei to determine if diminished excitability of these neurons *ex vivo* correlate with the ability of a traditional volatile GA such as isoflurane to induce hypnosis in mice. These experiments addressed a long-standing unresolved issue of whether inhibition of $\text{Ca}_v3.1$ T-channels in different functional

regions of the thalamus is important for GA-induced hypnosis. Most thalamic neurons fire APs in a regular (tonic) mode when depolarized from the resting membrane potential, and high frequency burst firing mode that crowns low-threshold calcium spikes (LTS) if they are hyperpolarized sufficiently to de-inactivate T-type calcium channels [11, 28]. Indeed, we showed that knocking down $\text{Ca}_v3.1$ channels in thalamus completely abolished LTS and greatly diminished rebound burst firing pattern while it had only a minimal effect on the tonic firing pattern (Figure 3). Our voltage- and current-clamp experiment validated our silencing technique using an shRNA approach that we also used to study the functional

role of $\text{Ca}_v3.1$ channel in the subiculum [20]. A previous study used a global knockout mouse to investigate the role of $\text{Ca}_v3.1$ channels in anesthetic sensitivities. Petrenko and colleagues reported that global $\text{Ca}_v3.1$ KO mice showed no change in anesthetic requirements (isoflurane, halothane, sevoflurane, pentobarbital) for LORR and LOWR but have delay in the onset of anesthetic induction measured by TTLORR [29]. They further concluded that the timely induction of anesthesia/hypnosis by volatile anesthetic agents and some intravenous anesthetic agents may require the normal functioning of the $\text{Ca}_v3.1$ channel isoform. However, since $\text{Ca}_v3.1$ channels are expressed in many different parts of the thalamus, hippocampus and cortex, we opted for the knock-down approach to be able to target specific thalamic regions and minimize compensatory changes in neuronal circuitry that are more likely with global knockouts. In contrast to this study with global KO mice, we found that knocking down this T-channel isoform in MIT leads to a decreased requirement for hypnosis induced by isoflurane. Our finding is consistent with another study that examined the specific role of the VB and CMT in anesthetic hypnosis [6]. Specifically, Baker and colleagues recorded local field potentials (LFPs) from four brain regions (barrel neocortex, VB, anterior cingulate cortex, and CMT) simultaneously in freely moving rodents during transitions into natural sleep and anesthetic-induced (propofol and dexmedetomidine) LORR. They found that for propofol-induced LORR and natural sleep, the LFP changes with neuronal oscillations occur first in the nonspecific thalamus before changes could be detected in the neocortex. With dexmedetomidine, they found that initial LFP changes occurred simultaneously in the nonspecific thalamus and neocortex. Overall, they concluded that CMT acts as key hub through which both anesthetic hypnosis and natural sleep are initiated. Our results are consistent with the idea that the nonspecific MIT region of the thalamus is more important for isoflurane-induced hypnosis than the specific sensory VB thalamus. In addition, we validated important role of $\text{Ca}_v3.1$ isoform of T-type channels in this mechanism of anesthetic hypnosis. Towards this end, we recently reported that other classes of GAs like neuroactive steroids induce hypnosis in rodents at least in part by inhibiting $\text{Ca}_v3.1$ channels in the thalamus [30, 31]. Hence, our future experiments will address the issue if $\text{Ca}_v3.1$ T-type channels in MIT region of the thalamus show a similar preferential role in neurosteroid-induced hypnosis.

Author contributions

Conceptualization, TTS and SMT; analysis, TTS; experiment, TTS, SF, BF-R, VT; writing—original draft preparation, SMT; writing—review and editing, TTS, SF, BF-R, VT; supervision, SMT; funding acquisition, TTS and SMT.

Data availability

The raw data supporting the conclusions of this article will be made available by the authors, without undue reservation.

Ethics statement

Experimental procedures with animals were performed according to the guidelines approved by the Institutional Animal Care and Use Committee (IACUC) of the University of Colorado Anschutz Medical Campus. Treatments of animals adhered to guidelines set forth in the NIH Guide for the Care and Use of Laboratory Animals. Our study was approved by the ethics committee of the University of Colorado Anschutz Medical Campus.

Funding

The author(s) declare that financial support was received for the research and/or publication of this article. This study was funded in part by grants from the National Institutes of Health (GRANT# GM141802 and VA Merit I01BX004763 to SMT and DA055258 to TTS) and funds from the Department of Anesthesiology and School of Medicine at Anschutz Medical Campus.

Acknowledgments

We thank MacKenzie Walz and Sarah Kawell for maintaining the mouse colonies.

Conflict of interest

The author(s) declared no potential conflicts of interest with respect to the research, authorship, and/or publication of this article.

Generative AI statement

The authors declare that no Generative AI was used in the creation of this manuscript.

References

1. Franks NP. General anaesthesia: from molecular targets to neuronal pathways of sleep and arousal. *Nat Rev Neurosci* (2008) **9**:370–86. doi:10.1038/nrn2372
2. Herold KF, Sanford RL, Lee W, Andersen OS, Hemmings HC. Clinical concentrations of chemically diverse general anesthetics minimally affect lipid bilayer properties. *Proc Natl Acad Sci* (2017) **114**:3109–14. doi:10.1073/pnas.1611717114
3. Orestes P, Todorovic SM. Are neuronal voltage-gated calcium channels valid cellular targets for general anesthetics? *Channels (Austin)* (2010) **4**:518–22. doi:10.4161/chan.4.6.12873
4. Vertes RP, Linley SB, Hoover WB. Limbic circuitry of the midline thalamus. *Neurosci and Biobehavioral Rev* (2015) **54**:89–107. doi:10.1016/j.neubiorev.2015.01.014
5. Vertes RP, Linley SB, Rojas AKP. Structural and functional organization of the midline and intralaminar nuclei of the thalamus. *Front Behav Neurosci* (2022) **16**:964644. doi:10.3389/fnbeh.2022.964644
6. Baker R, Gent TC, Yang Q, Parker S, Vyssotski AL, Wisden W, et al. Altered activity in the central medial thalamus precedes changes in the neocortex during transitions into both sleep and propofol anesthesia. *The J Neurosci* (2014) **34**:13326–35. doi:10.1523/jneurosci.1519-14.2014
7. Alkire MT, Haier RJ, Fallon JH. Toward a unified theory of narcosis: brain imaging evidence for a thalamocortical switch as the neurophysiologic basis of anesthetic-induced unconsciousness. *Conscious Cogn* (2000) **9**:370–86. doi:10.1006/cog.1999.0423
8. Joksovic PM, Nelson MT, Jevtovic-Todorovic V, Patel MK, Perez-Reyes E, Campbell KP, et al. Cav3.2 is the major molecular substrate for redox regulation of T-type Ca²⁺ channels in the rat and mouse thalamus. *The J Physiol* (2006) **574**:415–30. doi:10.1113/jphysiol.2006.110395
9. Talley EM, Cribbs LL, Lee JH, Daud A, Perez-Reyes E, Bayliss DA. Differential distribution of three members of a gene family encoding low voltage-activated (T-type) calcium channels. *J Neurosci* (1999) **19**:1895–911. doi:10.1523/jneurosci.19-06-01895.1999
10. Kim D, Song I, Keum S, Lee T, Jeong MJ, Kim SS, et al. Lack of the burst firing of thalamocortical relay neurons and resistance to absence seizures in mice lacking $\alpha 1G$ T-type Ca²⁺ channels. *Neuron* (2001) **31**:35–45. doi:10.1016/s0896-6273(01)00343-9
11. Timic ST, Feseha S, Valdez R, Zhao W, Klawitter J, Todorovic SM. Alterations in oscillatory behavior of central medial thalamic neurons demonstrate a key role of Cav3.1 isoform of T-channels during isoflurane-induced anesthesia. *Cereb Cortex* (2019) **29**:1–18. doi:10.1093/cercor/bhz002
12. Timic Stamenic T, Manzella FM, Maksimovic S, Krishnan K, Covey DF, Jevtovic-Todorovic V, et al. Further evidence that inhibition of neuronal voltage-gated calcium channels contributes to the hypnotic effect of neurosteroid analogue, 3 β -OH. *Front Pharmacol* (2022) **13**:850658. doi:10.3389/fphar.2022.850658
13. Alkire MT, Asher CD, Franciscus AM, Hahn EL. Thalamic microinfusion of antibody to a voltage-gated potassium channel restores consciousness during anesthesia. *Anesthesiology* (2009) **110**:766–73. doi:10.1097/aln.0b013e31819c461c
14. Lioudyno MI, Birch AM, Tanaka BS, Sokolov Y, Goldin AL, Chandy KG, et al. Shaker-related potassium channels in the central medial nucleus of the thalamus are important molecular targets for arousal suppression by volatile general anesthetics. *The J Neurosci* (2013) **33**:16310–22. doi:10.1523/jneurosci.0344-13.2013
15. Alkire MT, McReynolds JR, Hahn EL, Trivedi AN. Thalamic microinjection of nicotine reverses sevoflurane-induced loss of righting reflex in the rat. *Anesthesiology* (2007) **107**:264–72. doi:10.1097/01.anes.0000270741.33766.24
16. Ren S, Wang Y, Yue F, Cheng X, Dang R, Qiao Q, et al. The paraventricular thalamus is a critical thalamic area for wakefulness. *Science* (2018) **362**:429–34. doi:10.1126/science.aat2512
17. Colavito V, Tesoriero C, Wirtu AT, Grassi-Zucconi G, Bentivoglio M. Limbic thalamus and state-dependent behavior: the paraventricular nucleus of the thalamic midline as a node in circadian timing and sleep/wake-regulatory networks. *Neurosci and Biobehavioral Rev* (2015) **54**:3–17. doi:10.1016/j.neubiorev.2014.11.021
18. Joksovic PM, Todorovic SM. Isoflurane modulates neuronal excitability of the nucleus reticularis thalami *in vitro*. *Ann New York Acad Sci* (2010) **1199**:36–42. doi:10.1111/j.1749-6632.2009.05172.x
19. Eckle VS, DiGrucio MR, Uebele VN, Renger JJ, Todorovic SM. Inhibition of T-type calcium current in rat thalamocortical neurons by isoflurane. *Neuropharmacology* (2012) **63**:266–73. doi:10.1016/j.neuropharm.2012.03.018
20. Joksimovic SM, Ghodsi SM, Heinsbroek JA, Orfila JE, Busquet N, Tesic V, et al. Cav3.1 T-type calcium channels are important for spatial memory processing in the dorsal subiculum. *Neuropharmacology* (2023) **226**:109400. doi:10.1016/j.neuropharm.2022.109400
21. Gangadharan G, Shin J, Kim S-W, Kim A, Paydar A, Kim D-S, et al. Medial septal GABAergic projection neurons promote object exploration behavior and type 2 theta rhythm. *Proc Natl Acad Sci* (2016) **113**:6550–5. doi:10.1073/pnas.1605019113
22. Todorovic SM, Lingle CJ. Pharmacological properties of T-type Ca²⁺ current in adult rat sensory neurons: effects of anticonvulsant and anesthetic agents. *J Neurophysiol* (1998) **79**:240–52. doi:10.1152/jn.1998.79.1.240
23. Feseha S, Timic Stamenic T, Wallace D, Tamag C, Yang L, Pan JQ, et al. Global genetic deletion of Cav3.3 channels facilitates anaesthetic induction and enhances isoflurane-sparing effects of T-type calcium channel blockers. *Sci Rep* (2020) **10**:21510–0. doi:10.1038/s41598-020-78488-8
24. Schiff ND. Central thalamic contributions to arousal regulation and neurological disorders of consciousness. *Ann New York Acad Sci* (2008) **1129**:105–18. doi:10.1196/annals.1417.029
25. Crunelli V, David F, Leresche N, Lambert RC. Role for T-type Ca²⁺ channels in sleep waves. *Pflügers Archiv - Eur J Physiol* (2014) **466**:735–45. doi:10.1007/s00424-014-1477-3
26. Vertes RP, Hoover WB, Rodriguez JJ. Projections of the central medial nucleus of the thalamus in the rat: node in cortical, striatal and limbic forebrain circuitry. *Neuroscience* (2012) **219**:120–36. doi:10.1016/j.neuroscience.2012.04.067
27. Vertes RP, Hoover WB. Projections of the paraventricular and paratenial nuclei of the dorsal midline thalamus in the rat. *J Comp Neurol* (2008) **508**:212–37. doi:10.1002/cne.21679
28. Stamenic TT, Todorovic SM. Cytosolic ATP relieves voltage-dependent inactivation of T-type calcium channels and facilitates excitability of neurons in the rat central medial thalamus. *eNeuro* (2018) **5**:ENEURO.0016–8.2018. doi:10.1523/eneuro.0016-18.2018
29. Petrenko AB, Tsujita M, Kohno T, Sakimura K, Baba H. Mutation of $\alpha 1GT$ -type calcium channels in mice does not change anesthetic requirements for loss of the righting reflex and minimum alveolar concentration but delays the onset of anesthetic induction. *Anesthesiology* (2007) **106**:1177–85. doi:10.1097/01.anes.0000267601.09764.e6
30. Timic Stamenic T, Feseha S, Manzella FM, Wallace D, Wilkey D, Corrigan T, et al. The T-type calcium channel isoform Cav3.1 is a target for the hypnotic effect of the anaesthetic neurosteroid (3 β ,5 β ,17 β)-3-hydroxyandrostane-17-carbonitrile. *Br J Anaesth* (2021) **126**:245–55. doi:10.1016/j.bja.2020.07.022
31. Manzella FM, Cabrera OH, Wilkey D, Fine-Raquet B, Klawitter J, Krishnan K, et al. Sex-specific hypnotic effects of the neuroactive steroid (3 β ,5 β ,17 β)-3-hydroxyandrostane-17-carbonitrile are mediated by peripheral metabolism into an active hypnotic steroid. *Br J Anaesth* (2023) **130**:154–64. doi:10.1016/j.bja.2022.09.025